Influence of Initial Conditions and Climate Forcing on Predicting Arctic Sea Ice

E. Blanchard-Wrigglesworth,[1] C. M. Bitz,[1] and M. M. Holland,[2]

E. Blanchard-Wrigglesworth, Department of Atmospheric Sciences, University of Washington, Seattle, WA 98195-1640, USA. (ed@atmos.washington.edu)

C. M. Bitz, Department of Atmospheric Sciences, University of Washington, Seattle, WA 98195-1640, USA

M. M. Holland, National Center for Atmospheric Research, Boulder, CO, 80307-3000, USA.

[1]Department of Atmospheric Sciences, University of Washington, Seattle, Washington, USA.

[2]National Center for Atmospheric Research, Boulder, Colorado, USA.

The recent sharp decline in Arctic sea ice has triggered an increase in the interest of Arctic sea ice predictability, not least driven by the potential of significant human industrial activity in the region. In this study we quantify how long Arctic sea ice predictability is dominated by dependence on its initial conditions versus dependence on its secular decline in a state-of-the-art global circulation model (GCM) under a 'perfect model' assumption. We demonstrate initial-value predictability of pan-Arctic sea ice area is continuous for 1-2 years, after which predictability is intermittent in the 2-4 year range. Predictability of area at these longer lead times is associated with strong area-thickness coupling in the summer season. Initial-value predictability of pan-Arctic sea ice volume is significant continuously for 3-4 years, after which time predictability from secular trends dominates. Thus we conclude predictability of Arctic sea ice beyond 3 years is dominated by climate forcing rather than initial conditions. Additionally, we find that forecast of summer conditions are equally good from the previous September or January initial conditions.

1. Introduction

Predicting Arctic sea ice has long been practiced by elders of Inuit communities in the Arctic, whose livelihoods depend on sea ice for travel and hunting [*Fox*, 2003]. There is increasing interest in predicting Arctic sea ice among shipping and resource extraction industries, spurred in part by the recent sharp decline of Arctic sea ice area, particularly in summer [*Serreze et al.*, 2007]. For example, advanced knowledge of the opening of the northwest and northeast passages could offer faster and cheaper travel between the Atlantic and Pacific oceans [*ACIA*, 2004].

The persistence of anomalies in Arctic sea ice area has multiple important timescales [*Blanchard-Wrigglesworth et al.*, 2011]. There is an initial exponential decay of the lagged correlation from a given month that results in a negligible correlation after 2-4 months. For example, correlation of Arctic sea ice area anomalies in May with successive months is essentially zero by September. Beyond this initial loss of persistence, there is a reemergence that occurs in some seasons owing to coupled interactions between sea ice area anomalies, thickness anomalies (which tend to persist much longer than area anomalies), and sea surface temperature (SST) anomalies. The reemergence is observed in nature, but it is more pronounced in a GCM analyzed in the study.

Global Climate Models (GCMs) have been employed to assess the prognostic predictability of Arctic sea ice in a few studies by using 'perfect model' approach in which ensemble integrations are initialized from a reference model integration. Such studies neglect errors from imperfect knowledge of the initial state and therefore give the upper limit of predictability for the model. One study found central Arctic thickness predictability for 2 years, while Arctic sea ice area predictability was only better than expected from damped persistence for a few months near the ice edge [*Koenigk and Mikolajewicz*, 2009]. Another found sea ice area in a year with above average thickness generally exhibits longer predictability than in a year with below average thickness [*Holland et al.*, 2010]. These studies are valuable precursors to practical GCM predictions but they have only evaluated predictability from initial conditions ('predictability of the first kind'- *Lorenz* [1975]). This 'initial-value' predictability is measured by comparing the time evolution of the spread of an ensemble forecast distribution to its asymptotic limit.

Predictability from changing boundary conditions ('predictability of the second kind'- *Lorenz* [1975]), such as results from anthropogenic climate forcing, could be very important for a system whose mean state is rapidly changing, as is the case for Arctic sea ice. This 'forced' predictability results in a transient in the ensemble mean of an ensemble forecast distribution. A question of interest is how long initial-value predictability dominates over forced predictability in sea ice, or is there a gap when there is no predictability. A similar question has been explored for Pacific upper ocean temperatures, which showed within 5-8 years predictability from climate forcings exceeds that from initial values [*Branstator and Teng*, 2010]. We assess the 'forced' predictability in sea ice through the use of relative entropy [*Kleeman*, 2002] from information theory, which has recently been applied in the context of oceanic temperature predictability [*Teng and Branstator*, 2010].

2. Methods

We investigate predictability of pan-Arctic sea ice area and volume in perfect model studies with the Community Climate System Model version 4 (CCSM4) [*Gent et al.*, 2011] at 1° resolution in all components. Because persistence of Arctic sea ice area varies seasonally [*Blanchard-Wrigglesworth et al.*, 2011], we designed our experiments to assess initializations from two different times of the year as noted in table 1. The start times were chosen to capture times near the maximum and minimum of sea ice area persistence. We conduct an ensemble of prediction experiments (EPEs) for each start time composed of 60 runs with initial conditions drawn from six different 20^{th} Century integrations (see *Meehl et al.* Submitted, and table 1). We refer to runs with initial conditions from the same start time and 20th century integration as a set. Each set has either 8 or 20 members of 2 or 5 years in length (as noted in table 1), and all members of the set have the same sea ice, land, and ocean initial conditions. The set members are unique in their atmospheric initial conditions, which are drawn from consecutive days centered on 1 January or September. Given the rapid adjustment time scales of the atmosphere, each member of a set can be considered independent. All integrations have time-varying, radiative forcing [*Gent et al.*, 2011]. We find that the varying number of members in the sets in the first two years does not distort our results (see auxiliary materials).

We use monthly model output for all our computations. Anomalies are calculated as the departure from the mean of each set. A time-evolving standard deviation (σ) is computed from the anomalies across each January and September EPE. We use years 1996–2005 of the six 20th century integrations to construct statistics of a ‘reference’ distribution, which we assume has no memory of its initial conditions in 1850. The time-evolving mean (or trend) of the reference distribution is estimated from a linear fit to the ensemble mean of the six runs. The reference σ is estimated from anomalies of this time-evolving mean.

In the reference, σ is assumed to be monthly varying but annually periodic, a reasonable assumption for the shortness of the period considered. All significance values are stated at the 95% confidence interval.

Satellite observations of sea ice area [*Fetterer et al.*, 2002, updated 2010] from 1979-2010 are used to compute the trends and standard deviation of observed sea ice area.

3. Results

Forecast accuracy is a user defined concept with no universally defined skill standard [*Collins*, 2002], so we consider several measures. We begin by evaluating the growth of the cross-ensemble standard deviation (or ensemble spread) of each EPE, which addresses initial-value predictability only, using the Root Mean Square Deviation (RMSD, also known as Root Mean Square Error). The RMSD is defined as

$$RMSD = \sqrt{\frac{1}{N}\sum_{j=1}^{6}\sum_{i=1}^{8,20}\sum_{k\neq i}(x_{kj} - x_{ij})^2}, \tag{1}$$

where x_{ij} is either pan-Arctic sea ice area or volume (henceforth refered to as just area or volume) and the indexes j indicates the set, i indicates ensemble member, and N the total number of variables in the summation minus 1 [see *Collins* 2002]. We note that our interpretation of the RMSD is in close agreement with those from the Prognostic Potential Predictability (PPP) [*Pohlmann et al.*, 2004] and growth of the standard deviation of the EPE (see auxiliary materials).

Figure 1 shows the RMSD for area and volume for January and September EPEs. An RMSD of zero indicates perfect predictability, and the reference RMSD is the limit above which there is no predictability. Predictability is considered significant when the RMSD of the EPE is less than that of the reference judged using an F-test. As expected from its shorter persistence timescale, the initial-value predictability is lower for area than for volume. The time it takes for the RMSD for area to first lose significance is about 1.5–2 years (Fig. 1a,c). Beyond 2 years the RMSD for area is significant only intermittently, with a tendency for significance to recur in some months, notably May–July and September–October of years 3 and 4. After 4 years all initial-value predictability of area is lost. For sea ice volume, the initial-value predictability of each EPE is significant continuously for 3–4 years (Fig. 1b,d).

We compare the RMSD for each EPE to an estimate from an autoregressive process of order 1 (AR1 model, see, e.g., *vonStorch and Zwiers* [1999]) — an estimate of the predictability from damped persistance alone. The AR1 model is based on the one-lag correlation (a) and variance (σ^2) of the control for the month following the start time (e.g., for the January start, a is for January correlated with February and σ is for only the month of January). Hence, the asymptotic limit of the AR1 model RMSD approaches that of the reference for the start month. The parameters a and σ for area vary strongly with season [*Blanchard-Wrigglesworth et al.*, 2011], so the AR1 model RMSD for area should only be considered relevant for the first few months. The initial rapid rise of the AR1 model RMSD for area for the September EPE is due to both a low a and high σ. In other words, damped persistence alone from September conditions offers poor predictability — much worse than from January. However, the EPE predictability is just as good for September as January start times (based on comparing the RMSD of EPEs and reference at similar lead times), which offers hope that prognostic predictions of area can beat simple damped persistence at least for a few months of lead time.

Initial value predictability for January and September EPEs is generally indistinguishable in spring of the first year for both area and volume, as evident by the similar magnitude of RMSD in Fig. 1e and f. This season leads to a period of enhanced growth in the RMSD of the area and volume distributions that recurs in June–July each year. It is perhaps not a coincidence that initial-value predictability should decline at a time of high solar insolation, when snow cover disappears, surface albedo drops sharply, and atmospheric perturbations have been shown to produce the greatest variation in sea ice volume [*Bitz et al.*, 1996]. We emphasize that the decline does not result in complete loss of predictability, at least not until several years have passed.

Our previous work showed that sea ice area anomalies could disappear and reemerge by association with long-lived thickness anomalies during the summer season [*Blanchard-Wrigglesworth et al.*, 2011]. Such phenomena are possible if thickness and area anomalies are only strongly correlated in summer and the area anomaly decays in fall while the thickness anomaly in the central Arctic persists all year. Volume is the hemispheric integral of local thickness weighted by the local fractional sea ice cover. Thus volume is strongly related to central Arctic thickness. Figure 2 shows that sea ice area and volume are indeed strongly correlated only in summer in both EPE and control. We thus expect that negligible area predictability in spring followed by reemergence of area predictability in summer-fall (e.g., see fig. 1a and c in 2002 and 2003) is a result of coupling between the slowly-varying volume and the generally faster-varying area. While we do see winter area predictability lasts up to 3 years, this is not imparted by volume anomalies, but presumably originates from persistence in the ocean model component. Further evidence of the controlling influence of volume on area is that once the EPE RMSD becomes undistinguishable from the reference RMSD in the 5th year (see fig. 1 b and d), area loses all initial-value predictability (see fig. 1 a and c).

Next we consider how the rapid decline in area and volume affect predictability through analysis of relative entropy, which measures the information (in bits) provided by a prediction over the climatology [*Kleeman*, 2002]. The univariate form of relative entropy is defined as

$$RE = \frac{1}{2}[ln(\frac{\sigma_c^2}{\sigma_e^2}) + \frac{\sigma_e^2}{\sigma_c^2} + \frac{(\mu_e - \mu_c)^2}{\sigma_c^2} - 1], \tag{2}$$

where σ_c and σ_e are standard deviations of the control and experiment respectively, and μ_c and μ_e is the mean of the control and experiment respectively. We refer to the first two and fourth terms in equation 2 as the *dispersion* component and the third term as the *signal* component of the relative entropy. Relative entropy evaluates both the predictability of the spread (dispersion) and the evolution of the mean (signal) of the EPE distribution. The initial-value predictability has both dispersion and signal components, while the forced predictability affects only the signal component in the timeframe of our experiments. We estimate a null hypothesis lower (rejection) level by calculating the relative entropy with respect to the control of a synthetic data set whose mean and standard deviation are constructed to be minimally significantly different from the control at exactly the 95% level (see auxiliary materials).

From the relative entropy of the EPEs (see Figure 3), we see that most of the initial-value predictive information in volume is a result of the dispersion component of the ensemble, which provides predictability for about 3-4 years (in agreement with Fig. 1).

The signal component also yields initial-value predictability in volume, which is much smaller than the dispersion component during the first year, but comparable in years 2-3, particularly in the September EPE. All initial-value predictability for volume disappears by year 5. The forced predictability of volume becomes comparable with initial-value predictability in year 3, and forced predictability exceeds initial-value predictability in year 4. For volume, the sum of initial-value and forced predictability is significant all 5 years, except for a brief period in the January EPE at the end of year 3.

For area, dispersion provides continuous initial-value predictability for 2 years, and then it is intermittently significant in years 3 and 4. Unlike volume, the greater contributor to initial-value predictability of area is from the signal component in the first 6 months and in the 2nd winter following the forecast start date. Given the more rapidly-varying, noisier nature of area compared to volume, it is harder to define a precise time at which all area initial-value predictability saturates (to use a term from *Branstator and Teng* [2010]), but saturation is beyond 2 years for the signal component and 4 years for the dispersion component. The first evidence of forced predictability in area does not appear until year 5, which is much later than for volume. Thus, there are extensive periods in the 2-5 year range where no significant total predictability is present.

4. Discussion and Conclusions

The evolution of volume and area in the 20^{th} Century runs for 2000-2005 (see table1) can be used as a window to the timescale for when forced predictability becomes significant. It takes only about 4 years for the volume to reach a new mean state (when the secular change exceeds -1 standard deviation), whereas for area it takes about 6 years. Unfortunately, the observational record of sea ice thickness is too incomplete to calculate this metric for observed sea ice volume, yet we note that recent trends [*Kwok and Rothrock*, 2009] are comparable to those in the model. Observed sea ice area retreat indicates it currently takes about about 5 years to reach a new mean state. The near agreement between the model and observations (where possible) supports the finding from our model results that at present predictability of the Arctic sea ice system beyond about 3-5 years is principally a boundary-forcing problem. In contrast, predictability for less than 3-5 years is an initial-value problem.

Area predictability is considerably longer than the predictability yielded by its inherent persistence timescale, in part due to the coupling of area and volume anomalies during the summer season. In the model there are times when no significant area predictability exists from either initial conditions or climate forcing, whereas for volume, significant predictability is present almost continuously. We find that beyond the spring, model predictions are equally good whether initialized in September or January, implying that in practice forecasts of the summer sea ice may be made as early as the fall.

Acknowledgments. We thank Grant Branstator, Joe Tribbia, Andrew Madja and Ben Kirtman for insightful discussions, and two anonymous reviewers for helpful comments. This research was supported by NSF PP grant ARC-0909313. Computing support was provided by NCAR's Computational and Information Systems Laboratory, sponsored by NSF.

References

ACIA (2004), Atmospheric circulation and Arctic sea ice in CCSM3 at medium and high resolution, *Impacts of a warming Arctic- Arctic climate impact assesment*, p. 144.

Bitz, C. M., D. S. Battisti, R. E. Moritz, and J. A. Beesley (1996), Low-frequency variability in the Arctic atmosphere, sea ice and upper-ocean climate system, *Journal of Climate*, *9*.

Blanchard-Wrigglesworth, E., K. Armour, C. M. Bitz, and E. deWeaver (2011), Persistence and inherent predictability of Arctic sea ice in a GCM ensemble and observations, *Journal of Climate*, *24* (1), doi:10.1175/2010JCLI3775.1.

Branstator, G., and H. Teng (2010), Two limits of initial-value decadal predictability in a CGCM, *Journal of Climate*, *23*, doi:10.1175/2010JCLI3678.1.

Collins, M. (2002), Climate predictability on interannual to decadal time scales: the initial value problem, *Climate Dynamics*, *19*, 671–692.

Fetterer, F., K. Knowles, W. Meier, and M. Savoie (2002, updated 2010), Sea ice index, *http://nsidc.org/data/go2135.html, accessed in April 2011*.

Fox, S. (2003), When the weather is uggianaqtuq: Inuit observations of environmental change, CD-ROM, *Boulder, CO: University of Colorado Geography Department Cartography Lab. Distributed by National Snow and Ice Data Center*.

Gent, P. R., G. Danabasoglu, L. Donner, M. Holland, E. Hunke, S. Jayne, D. Lawrence, R. Neale, P. Rasch, M. Vertenstein, P. Worley, Z.-L. Yang, and M. Zhang (2011), The Community Climate System Model version 4, *Journal of Climate*, *N/A*.

Holland, M. M., D. A. Bailey, and S. Vavrus (2010), Inherent sea ice predictability in the rapidly changing arctic environment of the Community Climate System Model, version 3, *Climate Dynamics*, doi:10.1007/s00382-010-0792-4.

Kleeman, R. (2002), Measuring dynamical prediction utility using relative entropy, *Journal of Atmospheric Sciences*, *59*, 2057–2072.

Koenigk, T., and U. Mikolajewicz (2009), Seasonal to interannual climate predictability in mid and high northern latitudes in a global coupled model, *Climate Dynamics*, *32*, doi:10.1007/s00382-008-0419-1.

Kwok, R., and D. A. Rothrock (2009), Decline in arctic sea ice thickness from submarine and Icesat records: 1958-2008, *Geophysical Research Letters*, *36*, doi: 10.1029/2009GL039035.

Lorenz, E. N. (1975), The physical bases of climate and climate modelling., in *Climate Predictability*, no. 16 in GARP, WMO.

Meehl, G. A., W. M. Washington, J. M. Arblaster, H. T. A. Hu, C. Tebaldi, W. G. Strand, and J. B. White III (Submitted), Climate system response to external forcings and climate change projections in CCSM4, *Journal of Climate*, *N/A*.

Pohlmann, H., M. Botzet, M. Latif, A. Roesch, M. Wild, and P. Tschuck (2004), Estimating the decadal predictability of a coupled AOGCM, *Journal of Climate*, *17*.

Serreze, M., J. Stroeve, and M. M. Holland (2007), Perspectives on the Arctic's shrinking sea-ice cover, *Science*, *315*(5818), doi:10.1126/science.1139426.

Teng, H., and G. Branstator (2010), Initial-value predictability of prominent modes of North Pacific subsurface temperature in a CGCM, *Climate Dynamics*, *24*, doi:

10.1007/s00382-010-0749-7.

vonStorch, H., and F. W. Zwiers (1999), *Statistical Analysis in Climate Research*, 484 pp., Cambridge University Press.

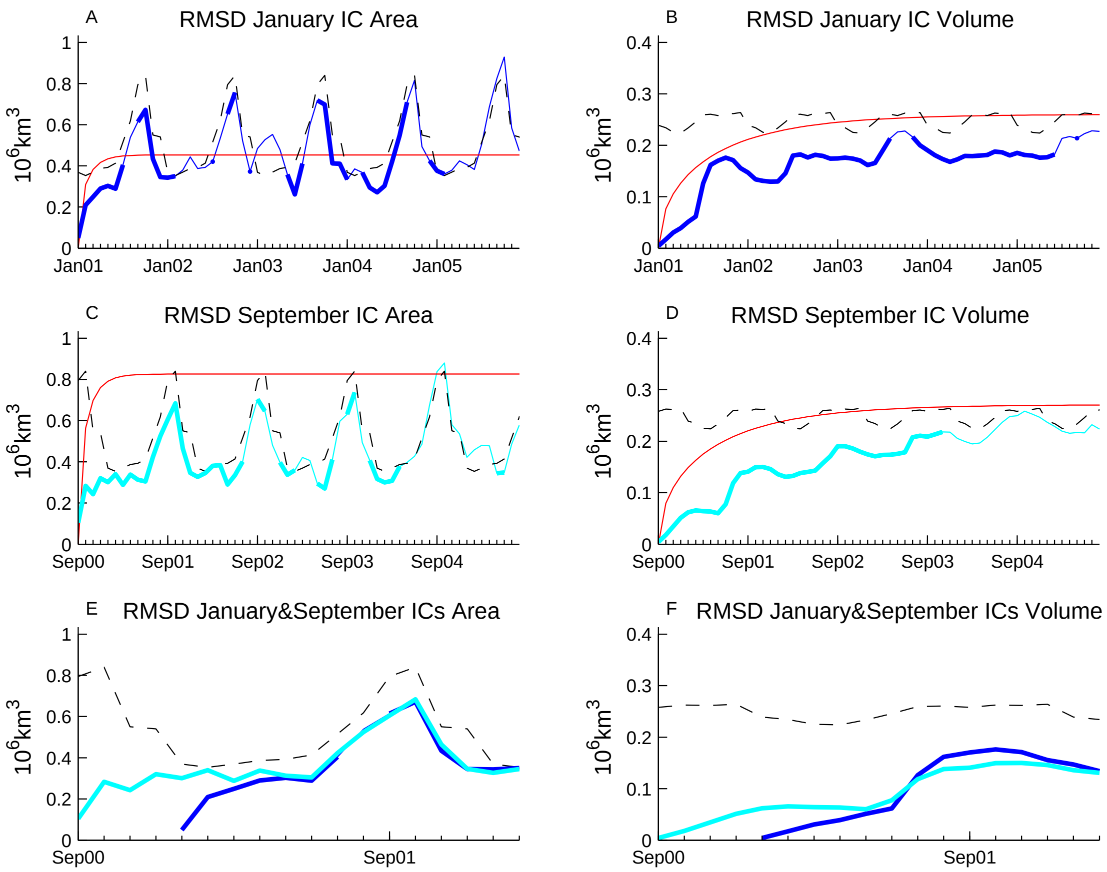

Figure 1. RMSD of Arctic sea ice volume and area for the January (dark blue) and September (light blue) EPEs. Estimates of RMSD from the reference integration (black dashed) indicate the limit of no predictability. The blue lines are heavy when the RMSD of the ensemble is significantly below the control RMSD. The red lines are the RMSD of an AR1 model, which provide a measure of the RMSD expected from persistence alone.

Table 1. Description of ensembles of prediction experiments

20^{th} Century run used for initialization	Starting times	Length of runs	Number of members
1	Sep 2000, Jan 2001	2 years	20
2	Sep 2000, Jan 2001	5 years	8
3	Sep 2000, Jan 2001	5 years	8
4	Sep 2000, Jan 2001	5 years	8
5	Sep 2000, Jan 2001	5 years	8
6	Sep 2000, Jan 2001	5 years	8

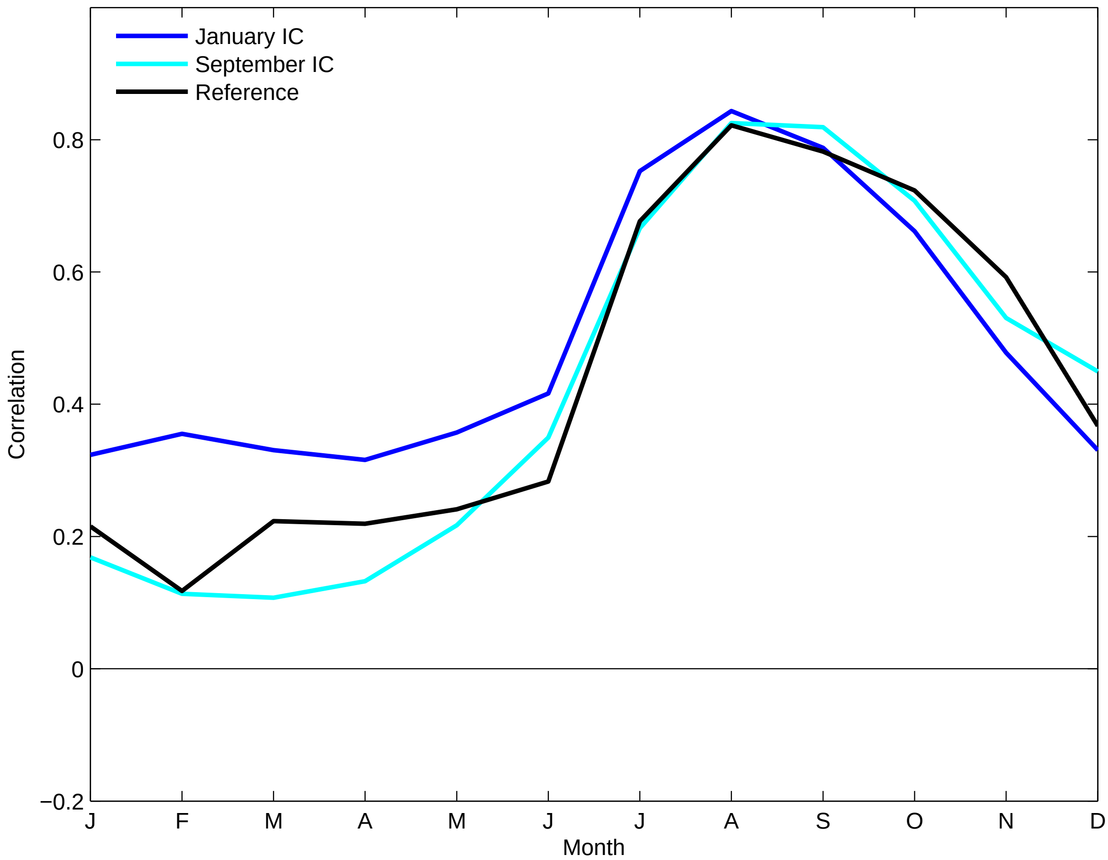

Figure 2. Correlation between area and volume anomalies. Monthly r values for January and September IC EPEs and reference run.

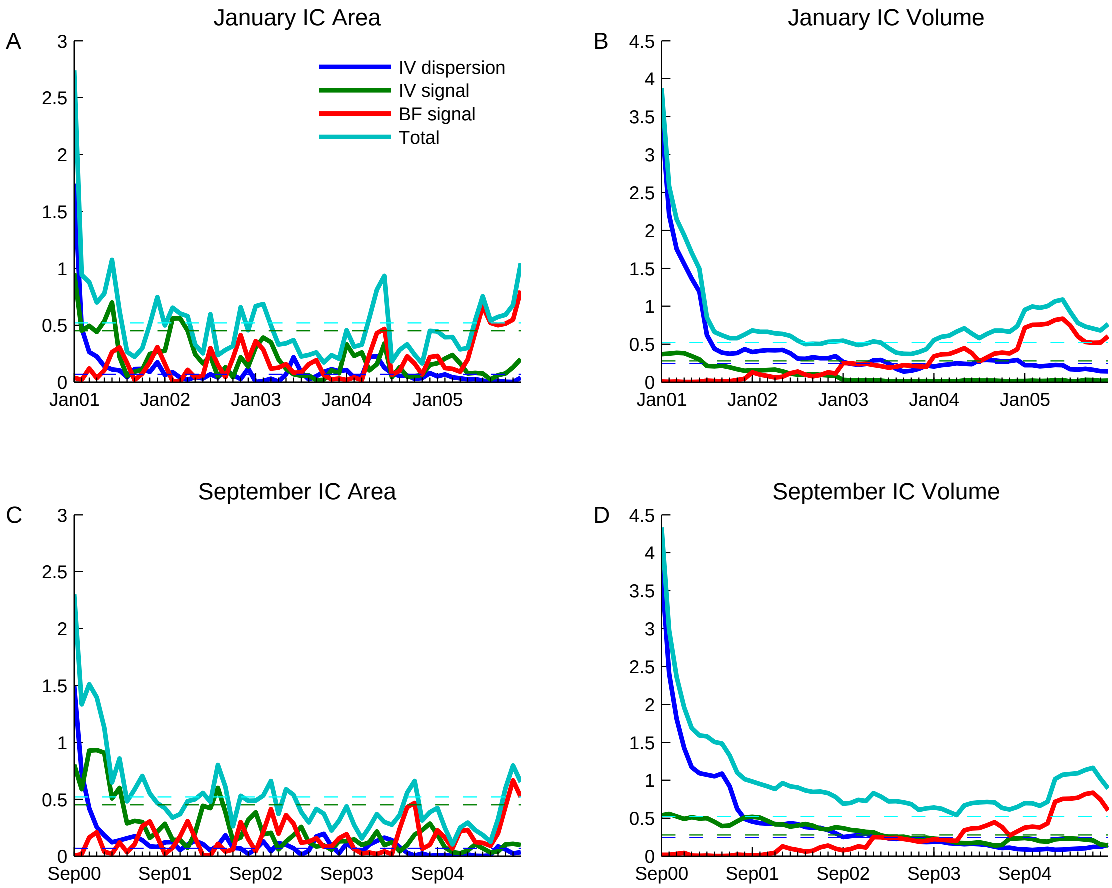

Figure 3. Relative entropy (unitless) of sea ice volume and area for January and September IC EPEs. The dashed lines represent the 95% null hypothesis rejection levels for dispersion (blue), signal (green) and total (cyan).